Effects of Interspecific Gene Flow on the Phenotypic Variance-Covariance Matrix in Lake Victoria Cichlids

Kay Lucek[1,2,3*], Lucie Greuter[1,2], Oliver M. Selz & Ole Seehausen[1,2]

[1] Department of Aquatic Ecology and Macroevolution, Institute of Ecology and Evolution, University of Bern, Baltzerstrasse 6, CH-3012 Bern, Switzerland
[2] Department of Fish Ecology and Evolution, EAWAG Swiss Federal Institute of Aquatic Science and Technology, Center of Ecology, Evolution and Biochemistry, Seestrasse 79, CH-6047 Kastanienbaum, Switzerland
[3] Department of Animal and Plant Sciences, University of Sheffield, Sheffield, S10 2TN, UK
* k.lucek@sheffield.ac.uk, 0041 31 631 30 16

Abstract

Quantitative genetics theory predicts adaptive evolution to be constrained along evolutionary lines of least resistance. In theory, hybridization and subsequent interspecific gene flow may however rapidly change the evolutionary constraints of a population and eventually change its evolutionary potential, but empirical evidence is still scarce. Using closely related species pairs of Lake Victoria cichlids sampled from four different islands with different levels of interspecific gene flow, we tested for potential effects of introgressive hybridization on phenotypic evolution in wild populations. We found that these effects differed among our study species. Constraints measured as the eccentricity of phenotypic variance-covariance matrices declined significantly with increasing gene flow in the less abundant species for matrices that have a diverged line of least resistance. In contrast we find no such decline for the more abundant species. Overall our results suggest that hybridization can change the underlying

phenotypic variance-covariance matrix, potentially increasing the adaptive potential of such populations.

Keywords: eccentricity, line of least resistance, hybridization, evolutionary constraints, P matrix

Acknowledgement

We thank Bänz Lundsgaard-Hansen, Blake Matthews, Joana Meier, Julia Schwarzer, Matthew McGee and Etienne Bezault for helpful discussions and comments on the manuscript. Two anonymous reviewers provided further constructive inputs. We acknowledge support from the Swiss National Science Foundation, grant 31003A_144046 to OS. KL is funded by a Swiss National Science Foundation Early Postdoc.Mobility grant P2BEP3_152103.

Introduction

Introgressive hybridization can promote or impede the progress of speciation and thus the emergence and maintenance of species diversity (Abbott et al., 2013). On one hand, hybridization may lead to the collapse of distinct species upon secondary contact or when selection regimes change (Seehausen et al., 1997; Taylor et al., 2006; Gilman & Behm, 2011; Vonlanthen et al., 2012; Rudman & Schluter, 2016). Conversely, hybridization may release lineages from constraining genetic correlations (Grant & Grant, 1994) increasing their evolvability (Parsons et al., 2011; Renaud et al., 2012; Seehausen et al., 2014; Selz et al., 2014; Stelkens et al., 2014, Figure 1), which may lead to the emergence of distinctively adapted hybrid populations that occupy a niche space different from either parental species (Rieseberg et al., 2003; Nolte et al., 2005; Mallet, 2007; Stelkens & Seehausen, 2009; Abbott et al., 2013).

Adaptation can be characterized as the movement of a population in phenotype space towards a local adaptive optimum, where the mean phenotype expressed in the population fits a given environment (Wright, 1932; Schluter, 2000; Orr, 2005; Calsbeek et al., 2011). Phenotypic evolution towards adaptive peaks is thought to be constrained along so called genetic "lines of least resistance" (LLR), which can be quantified as the leading eigenvector of the genetic variance-covariance matrix **G** (Lande, 1979; Schluter, 1996; Steppan et al., 2002; Klingenberg, 2010; Blows et al., 2015). The LLR is assumed to account for the largest proportion of heritable phenotypic variation and phenotypic evolution is predicted to be biased towards the direction of the LLR (Lande & Arnold, 1983; Schluter, 1996). The LLR is influenced by mutation, gene flow, drift and selection

(Lande, 1979; Steppan et al., 2002; Guillaume & Whitlock, 2007; Chapuis et al., 2008; Bailey et al., 2013). Selection may reorient the LLR towards the direction of the most prevalent selection regime (Lande, 1979; Schluter, 1996; 2000; Arnold et al., 2008) and gene flow may reorient the LLR towards that in the source population of gene flow (Guillaume & Whitlock, 2007).

In the absence of quantitative genetic data, the **G** matrix can be approximated by the **P** matrix (Cheverud, 1988), which is based on phenotypic data from wild populations (Arnold et al., 2008). **P** is thus defined as the combination of the genetic and environmental covariance matrices, that is **G** + **E** (Lande, 1979; Arnold & Phillips, 1999), where both effects could also interact (**G** x **E**; Falconer, 1989). Consequently, **P** matrices also include phenotypically plastic effects (Lande, 2009; Draghi & Whitlock, 2012; Wood & Brodie, 2015). Whereas many studies investigated the stability of the **P** matrix through time, and investigated whether evolution occurs along common LLRs in the **P** matrix (e.g. Schluter, 1996; Arnold et al., 2008; Eroukhmanoff & Svensson, 2008; Hine et al., 2009; Lucek et al., 2014a; 2014b), few studies have addressed to which degree gene flow may affect the **P** matrix and hence influence the evolutionary trajectory or potential of a population (Guillaume & Whitlock, 2007; Selz et al., 2014; Roseman, 2016). Theory suggests that gene flow between two diverged populations can change the shape of a **P** matrix, which is estimated by the eccentricity of the **P** matrix, i.e. the ratio of its two leading eigenvectors. Biologically, the degree of eccentricity is related to the extent of genetic constraints, where increased eccentricity reflects stronger covariation among traits while low eccentricities imply reduced covariance among traits and thus

fewer genetic constraints (Steppan et al., 2002; Jones et al., 2003; Eroukhmanoff & Svensson, 2011; Bailey et al., 2013). Gene flow may increase the phenotypic variance, leading to an increase (stronger covariation) or decrease (relaxed covariation) in eccentricity depending on whether or not gene flow increases variance along LLR or along other axes of the **P** matrix (Guillaume & Whitlock, 2007; Figure 1).

Here we use empirical data to test these predictions for the potential effects of gene flow on the **P** matrix. We study two sister species of African cichlid fish, *Pundamilia pundamilia* and *P. nyererei*, which co-occur at several islands in the southern part of Lake Victoria (Figure 2). Variation in water turbidity between islands is associated with different divergent selection regimes affecting *Pundamilia* species differentiation, with more gene flow between the sympatric species at islands with less clear water (Seehausen et al., 1997; 2008). Theory suggests that if the LLR have diverged between the *Pundamilia* species, hybridization should reduce the eccentricity of species specific **P** matrices (Guillaume & Whitlock, 2007). In contrast, if the *Pundamilia* species have not diverged in their LLR but rather differ in their mean position along a shared LLR, then gene flow between the two species should lead to an increase in species-specific eccentricity with increasing gene flow (Figure 1). When the species share the LLR and their mean trait values on the LLR, eccentricity may not change at all (Guillaume & Whitlock, 2007). We therefore first estimate if the *Pundamilia* species pair has diverged along a LLR or not at Makobe Island, being the island that is the least affected by recent changes in water turbidity and where there is no evidence for ongoing interspecific gene flow between the two

species (Seehausen et al., 2008). We then test the hypothesis that introgressive hybridization can relax genetic constraints in those parts of trait space where the two species are diverged in their LLR based on species-specific trait-by-trait **P** matrices.

We further illustrate the effects of gene flow in trait-by-trait **P** matrices on the multivariate phenotype in the context of the morphospace occupied by the most abundant species in the Makobe Island cichlid community (Seehausen et al., 1997; 2008). By including three additional sympatrically occurring species that represent other ecological guilds of the extant adaptive radiation of cichlids from Lake Victoria and together with the two Pundamilia species amount to ~80% of the local fish community in abundance (Seehausen & Bouton, 1997), we aim to put the potential effects of gene flow on *Pundamilia* phenotypes and **P** matrices into the community context of this adaptive radiation.

Material and Methods

Sampling

Cichlid fish were collected between 1993 and 1998 from four islands (Makobe, Python, Kissenda and Luanso) within the Mwanza Gulf in southern Lake Victoria (Figure 2). Each specimen was fixed in formaldehyde-solution immediately after capture and then transferred into an alcohol solution with increasing concentration (30, 50 and finally 70%). Individuals were identified to species level based on their morphology by OS. Only males of each species were used in this study as females cannot be unambiguously assigned to a species. At Luanso Island the two species cannot be distinguished genetically and only a single

phenotypically highly variable population of *Pundamilia* exists with some males resembling either of the species but most males being intermediate in phenotype (Seehausen *et al.*, 2008). They are consequently treated as a single, phenotypically variable population (*P.* "hybrid").

Morphological Analysis

For each individual, 13 linear morphological distances were measured to the nearest 0.01 mm using a digital caliper. Measurements were especially taken on the head to capture taxon specific ecological relevant trophic morphology (Barel *et al.*, 1977): head length (HL), lower jaw length (LJL), lower jaw width (LJW), snout length (SnL), preorbital depth (POD), cheek depth (ChD), eye length (EyL), eye depth (EyD), interorbital width (IOW), preorbital width (POW), snout width (SnW), body depth (BD) and standard length (SL). The latter was measured to size correct all other linear traits (see below). Many of these traits were found to have a heritable component in a common garden experiment using *Pundamilia* species from Kissenda Island (Magalhaes et al., 2009). Each fish was measured twice to estimate repeatability, which was generally >95% for all measurements (results not shown). For all further analyses the average of both independent measurements was used. Measurements, which were not reliable due to unusual body positions, were omitted. To account for potential size related effects and allometry, each measurement was first normalized by mean-scaling (Kirkpatrick, 2009), and subsequently regressed against standard length, retaining the residuals (Reist, 1986). To retain potential differences in trait means among populations, both the mean-scaling as well as the size correction was performed

combining all individuals from all populations. Missing data was replaced by the average trait value of a population after mean-scaling.

*Comparing **P** matrices*

For each *Pundamilia* population on each island the phenotypic variance-covariance (**P**) matrices of trait-by-trait morphospaces were calculated based on the size corrected residuals of the two traits. Using the 12 size corrected phenotypic traits, this resulted in 66 different trait-based pairwise **P** matrices per population. The eccentricity of each **P** matrix was then calculated as the ratio between the length of the orthogonal axes of the 95% confidence ellipsoid that account for the highest ($\mathbf{p}_{max}$) and lowest ($\mathbf{p}_{min}$) variance respectively (see Figure 1). Ellipses, $\mathbf{p}_{max}$ and $\mathbf{p}_{min}$ were calculated using a custom made script based on an implementation in the CAR package (Fox & Weisberg, 2011) in R 3.1.2 (R Development Core Team 2014).

To further test if species divergence may commonly involve a shared or a diverged LLR, trait-by-trait based **P** matrices were compared between *P. pundamilia* and *P. nyererei* from Makobe Island by calculating the pairwise differences in the intercept and the angle between the two leading eigenvectors of two **P** matrices. The latter is given as the inversed cosine of the dot product that is divided by the summed length of both eigenvectors (Schluter, 1996). The significances of these pairwise measurements were further established using a bootstrapping procedure with 1000 permutations (Berner, 2009). The two species were either considered to share a common LLR for a given trait-by-trait **P** matrix if neither the intercept nor the slope were significantly different (Figure

1a) or to deviate from a common LLR if the slope and/or the intercept differed significantly (Figure 1b-d). The eccentricity of trait-by-trait **P** matrices was furthermore calculated for each species at each island separately.

The degree of pairwise genetic divergence (F_{ST}) between sympatric *Pundamilia* species based on microsatellite loci was obtained for each pair from Seehausen et al. (2008) and subsequently used as a measure of gene flow between the two focal species at the different islands (Figure 2c). A linear mixed effect model was employed to test if eccentricity differs between the **P** matrices that have a diverged LLR and those that have a common LLR and if eccentricity is affected by gene flow (F_{ST}) and lastly if there is an interaction between either effect using island as a random factor. This analysis was separately performed for *P. pundamilia* and *P. nyererei* where in both cases the same set of hybrid individuals were included for Luanso Island.

Estimating the effects on the multivariate morphospace

In order to reconstruct the occupied multivariate morphospace of both *Pundamilia* species in relation to other cichlid species, the populations from Makobe Island showing the highest genetic divergence among our studied *Pundamilia* species-pairs (Seehausen et al. 2008) were used together with individuals from three other cichlid species present at Makobe Island, including the two most abundant ones ((Seehausen et al., 1998); *Mbipia mbipi, Neochromis omnicaeruleus* and *Paralabidochromis cyaneus*; see Table 1 for details). These species differ furthermore in their ecology: *P. pundamilia* feeds on benthic invertebrates, *P. nyererei* feeds predominantly on zooplankton, whereas *M. mbipi*

and *N. omnicaeruleus* feed predominantly on epilithic algae and *P. cyaneus* on insects and epilithic algae (Seehausen *et al.*, 1998).

The size corrected dataset was used to conduct a principal component analysis (PCA) using all individuals from all species from Makobe Island. The scores of the two leading PC axes were then compared among the five cichlid species using an ANOVA with a TukeyHSD *post hoc* test. To further infer where individuals from other islands would fall in the Makobe Island morphospace, they were subsequently projected into the Makobe morphospace following an approach described in (Selz et al., 2014; Lucek et al., 2014c). In short, this method takes the PC axes that were calculated using the Makobe Island individuals and subsequently infers where a given individual from another island would be placed in the mutli-species morphospace of Makobe Island. The PC scores of the projected *Pundamilia* species and the *Pundamilia* species at Makobe Island were subsequently compared using an ANOVA with *species* (*P. pundamilia, P. nyererei* or *P.* "hybrid" for Luanso Island) and *island* (Makobe and either Python, Kissenda or Luanso respectively) as factors. All analyses were performed in R.

Results

*Trait-by-trait **P** matrices*

Out of 66 pairwise trait comparisons between the two sympatric *Pundamilia* species at Makobe Island, 18 trait combinations show a significantly diverged LLR, especially involving lower jaw length (6 significant comparisons; Table S1), interorbital width and snout length (5 significant comparisons each; Figure S1;

Table S1). Out of these 18 cases, the angle between **P** matrices was significantly larger than zero on seven occasions whereas the remaining eleven cases showed a significant difference in the intercept (Figure S1; Table S1).

For *P. nyererei* we found that trait-by-trait **P** matrices with a LLR that both *Pundamilia* species at Makobe Island have in common, were at all islands more eccentric than matrices with diverged LLR ($F_{1,258}$ = 13.6, p < 0.001; Figure 3). Eccentricity in *P. nyererei* was however not affected by the extent of gene flow ($F_{1,258}$ = 0.1, p = 0.788), independent of whether LLR were shared with the sister species or diverged from it (a non-significant interaction between gene flow and divergence in the LLR; $F_{1,258}$ = 0.8, p = 0.385). For *P. pundamilia* on the other hand, **P** matrices with an LLR that both species at Makobe have in common, did not differ in their eccentricity from matrices with a diverged LLR at islands where gene flow is little, but in populations that have more gene exchange with the sister species, **P** matrices with diverged LLR lose their eccentricity as indicated by the significant interaction between F_{ST} and divergence in the LLR ($F_{1,258}$ = 6.0, p = 0.015).

Multivariate phenotypic changes

The two leading principal component (PC) axes for the overall morphospace, comprising five species of the Makobe Island community explained 73.2% of the total variation (63.6% and 9.6% on PC 1 and 2 respectively; Figure 4). Traits that accounted for most of the variation were LJL and LJW on the first and LJW and ChD on the second PC axis respectively (Table S2). Individual scores differed significantly among species along the first PC axis ($F_{4,154}$ = 198.1, p < 0.001),

where all pairwise *post hoc* comparisons were significant except for *P. pundamilia* and *M. mbipi* (Table S3). On the second PC axis species were significantly different too ($F_{4,154}$ = 24.7, p < 0.001), but only the comparisons involving *N. omnicaeruleus* yielded significant *post hoc* tests (Table S3).

When projecting *Pundamilia* from the other islands into the Makobe Island morphospace, the populations from Kissenda Island showed a slightly increased morphospace relative to those from Makobe (Figure 4), where their PC scores differed both between *species* ($F_{1,138}$ = 121.8, p < 0.001) and *island* ($F_{1,138}$ = 4.1, p = 0.044) along the first axis. In contrast, PC scores along the second axis differed only for the factor *island* ($F_{1,138}$ = 17.3, p < 0.001) but not *species* ($F_{1,138}$ = 1.6, p = 0.209). The *Pundamilia* populations from Python Island are more divergent from the Makobe populations, differing in their PC scores along the first and second axis for the factor *species* (PC1: $F_{1,129}$ = 56.1, p < 0.001, PC2: $F_{1,129}$ = 10.5, p = 0.002) and *island* (PC1: $F_{1,129}$ = 9.7, p = 0.002, PC2: $F_{1,129}$ = 49.5, p < 0.001). Lastly, the hybrid *Pundamilia* population from Luanso Island occupies a distinct part of the Makobe morphospace that matches the morphospace occupied by the ecologically distinct species *M. mbipi* in the Makobe community (Figure 4), where *M. mbipi* and *P.* "hybrid" specimens differ in their PC scores along the first ($F_{1,62}$ = 7.3, p = 0.009) but not the second ($F_{1,62}$ = 0.1, p = 0.870) axis. Lastly, the PC scores of the *Pundamilia* species at Makobe Island and the projected *P.* "*hybrid*" from Luanso differ along the first PC axis for the factor *species* ($F_{1,103}$ = 38.2, p < 0.001) and *island* ($F_{1,128}$ = 5.3, p = 0.023) but not on the second PC axis (*species*: $F_{1,103}$ = 0.7, p = 0.412; *island*: $F_{1,103}$ = 0.9, p = 0.352).

Discussion

Theory predicts the evolution of the genetic (**G**) and its related phenotypic (**P**) variance-covariance matrix to be constrained along so called lines of least resistances (LLRs; Schluter, 1996; Steppan et al., 2002; Eroukhmanoff, 2009; Klingenberg, 2010). Both **G** and **P** may change rapidly through drift, selection and gene flow (Lande, 1979; Steppan et al., 2002; Chapuis et al., 2008; Bailey et al., 2013). The role of gene flow between populations or introgressive hybridization between species has however been mainly studied in theory (Steppan *et al.*, 2002; Guillaume & Whitlock, 2007; Seehausen *et al.*, 2014). Here, we provide empirical data consistent with theoretical predictions for the effect of gene flow or introgressive hybridization on the **P** matrices in natural populations of cichlid sister species.

Our finding that more than two thirds of all trait-specific **P** matrices showed a shared LLR in the sympatric sister species pair of *Pundamilia pundamilia* and *P. nyererei* at Makobe Island is consistent with the idea that evolution is constrained by LLRs. This is expectation applies particularly in the early stage of species divergence (Schluter, 1996; 2000) and may thus be prominent in the evolutionary young Lake Victoria radiation of haplochromine cichlids (Seehausen, 2006). Over longer time, selection may overcome such constraints leading to an increased number of trait combinations that evolve diverged LLRs (Schluter, 2000; Eroukhmanoff, 2009). Introgressive hybridization can however rapidly release lineages from **G** matrix constraints and potentially increase the evolvability of the resulting hybrid population (Parsons et al., 2011; Renaud et al., 2012; Seehausen et al., 2014; Selz et al., 2014 ; Figure 1).

Interspecific gene flow may particularly affect the eccentricity of **P** matrices that have a diverged interspecific LLR, where a decreased level of eccentricity may reflect reduced trait covariation and hence a relaxation of former genetic constraints (Guillaume & Whitlock, 2007). Consistent with this, we observe in *P. nyererei* at all islands weaker eccentricity in **P** matrices with LLRs that have diverged in the sympatric sister species than those with common LLRs. This may be an effect of low levels of recent gene flow between the species or of gene flow in the past. Recent demographic analyses using whole genome sequence data have revealed that interspecific gene flow was predominantly from *P. nyererei* into *P. pundamilia* with much less gene flow into *P. nyererei* (Meier et al. *submitted*). It is possible that gene flow changes the eccentricity of the **P** matrix of an adapted population only when the migration rates are high (Guillaume & Whitlock, 2007). At the islands we studied, *P. pundamilia* is less abundant than its sister species *P. nyererei* (Seehausen & Bouton, 1997), which may explain the asymmetry of gene flow between the species (Meier et al., *submitted*).

Also consistent with theoretical predictions, we observe among *P. pundamilia* populations differences in **P** matrix eccentricity between populations that have received different amounts of interspecific gene flow from *P. nyererei* (Figure 3). Specifically **P** matrices that have LLRs that are diverged from those in the sister species are less eccentric at islands where *P. pundamilia* received more geneflow from *P. nyererei*, whereas LLRs that are shared between the species are more eccentric were gene flow was more common. Overall, *P. nyererei* shows an increased degree of phenotypic integration in comparison to *P. pundamilia*.

Because **P** matrices are based on phenotypic data from wild populations, changes in **P** may occur due to the combined effects of the genetic and environmental based covariance matrices, and their potential interactions (Lande, 1979; Falconer, 1989; Arnold & Phillips, 1999). Although many of the traits that we used to construct the trait-by-trait **P** matrices have been found to be rather heritable in a common garden experiment involving the same *Pundamilia* species as studied here (Magalhaes et al., 2009), it is possible that some part of the observed changes in the **P** matrix occurred due to phenotypic plasticity as a response to differences in the environment (Lande, 2009; Draghi & Whitlock, 2012; Wood & Brodie, 2015). Further laboratory experiments would thus be needed to estimate the actual differences in the genetic **G** matrix of our studied populations.

The differences in trait-by-trait **P** matrices that we found between the hybrid population at Luanso Island and the sister species at Makobe Island have implications for the multivariate phenotypes, which became apparent when projecting populations into the multivariate morphospace of the cichlid community at Makobe Island (Figure 4). Both *Pundamilia* species from Kissenda and Python Island still showed significant phenotypic divergence and occupied similar parts of the morphospace as their counterparts from Makobe Island, despite some degree of gene flow between them. By contrast, individuals from the hybrid population at Luanso Island do not fall into the full morphological space of the two putative original species. Instead, its morphospace occupation resembled that of another species at Makobe Island, *Mbipia mbipi*. Interestingly,

M. mbipi, the most abundant species in shallow waters of Makobe Island, is a shallow water omnivore that lives close to the rocks where it makes opportunistically use of gaps between the rocks and also feeds on the rock surfaces (Seehausen & Bouton 1997). The *Pundamilia* hybrids at Luanso occupy quite exactly the same spatial habitat (Seehausen 1997; Seehausen et al. 2008) and are also omnivorous. Lastly, at all three islands where the two *Pundamilia* species experience some degree of gene flow, some individuals lie outside the combined morphospace of the Makobe Island *Pundamilia* species. This may suggest that hybridization could lead to a relaxation of some genetic constraints and thus the expression of some novel phenotypes (Parsons et al., 2011; Renaud et al., 2012; Selz et al., 2014).

The quantitative genetic framework of **G** and its related **P** matrix has become a powerful tool to assess the genetic constraints to selection (Lande, 1979; Lande & Arnold, 1983; Schluter, 1996; Blows et al., 2015) and to study how selection, drift and gene flow may affect the evolution of a population (Chapuis et al., 2008; Bailey et al., 2013). Our findings are consistent with theoretical predictions (Chapuis et al., 2008; Bailey et al., 2013, Figure 1), suggesting that gene flow and introgessive hybridization can alter the **P** matrix of wild populations where the respective effect may depend on the relative abundance of hybridizing species and the level of interspecific gene flow. Such changes in the **P** matrix may potentially redirect a population towards a novel part of the morphospace and shift the **P** matrix towards a novel distinct adaptive peak (Seehausen et al., 2014).

Acknowledgement

We thank Bänz Lundsgaard-Hansen, Blake Matthews, Joana Meier, Julia Schwarzer, Matthew McGee and Etienne Bezault for helpful discussions and comments on the manuscript. Two anonymous reviewers provided further constructive inputs. We acknowledge support from the Swiss National Science Foundation, grant 31003A_144046 to OS. KL is funded by a Swiss National Science Foundation Early Postdoc.Mobility grant P2BEP3_152103.

Fi

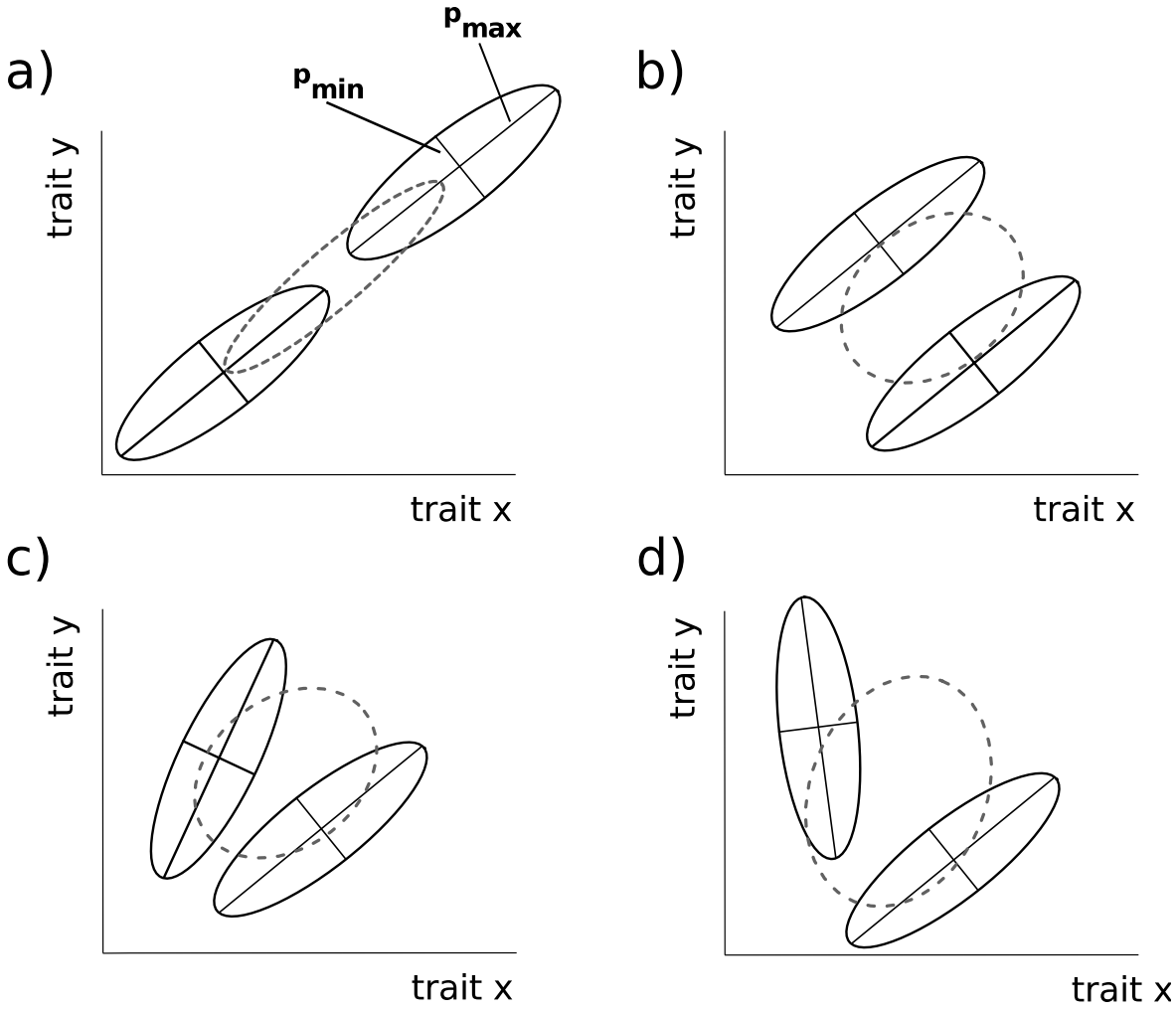

gure 1:

Schematic representation of different hybridization scenarios between species (solid outlined) and their respective potential outcomes (dashed lines): The outlined ellipses represent the 95% confidence ellipses of the phenotypic (**P**) variance/covariance matrices of two species. The lines indicate the direction of highest covariance ($\mathbf{p}_{max}$) and perpendicular to it the direction with lowest covariance ($\mathbf{p}_{min}$). The matrix is more constrained in phenotype space the higher $\mathbf{p}_{max}$ and the lower $\mathbf{p}_{min}$ is, which results in a more eccentric ellipse. In a) the **P** matrices of the two species are aligned along a common line of least resistance, with $\mathbf{p}_{max}$ having the same slope and the same intercept. Gene flow between

these two species should lead to an elongation of the **P** matrix because variance is increased along $\mathbf{p}_{max}$. In b) the two **P** matrices have still the same slope but their intercepts are different, in c) the opposite is the case, where the **P** matrices do not have the same slope but their intercepts are the same and in d) both intercept as well as slope are different between the matrices. The matrices in b), c) and d) all have diverged lines of least resistance therefore gene flow leads to **P** matrices which have a lower eccentricity because variance is increased along $\mathbf{p}_{min}$.

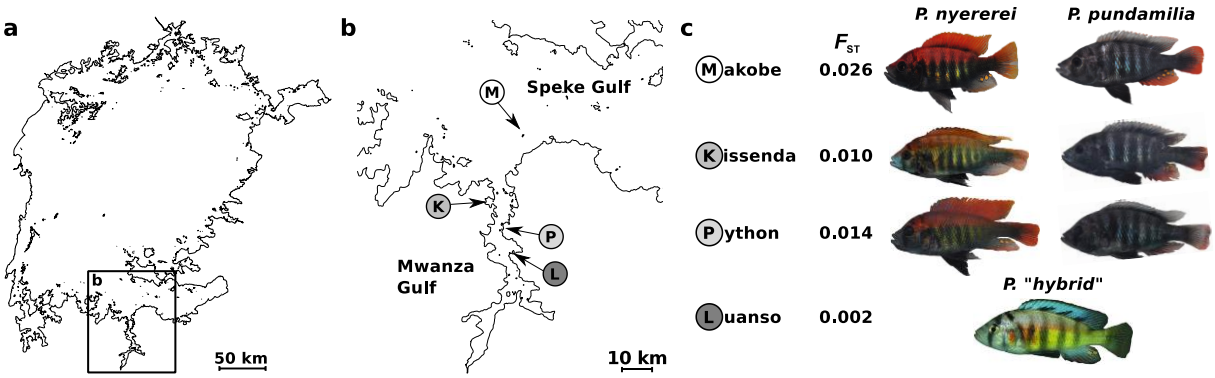

Figure 2

Overview of the studied populations: a) Map of Lake Victoria (Greg, 2015) . b) Detailed view of the Speke and Mwanza Gulf where the four islands Makobe, Kissenda, Python and Luanso are located. c) Male specimens of *Pundamilia nyererei* (left) and *P. pundamilia* (right) for each island. For Luanso, an exemplary specimen of the existing hybrid swarm is depicted. The pairwise F_{ST} – values between sympatric *Pundamilia* species are given for each island (taken from Seehausen et al. 2008).

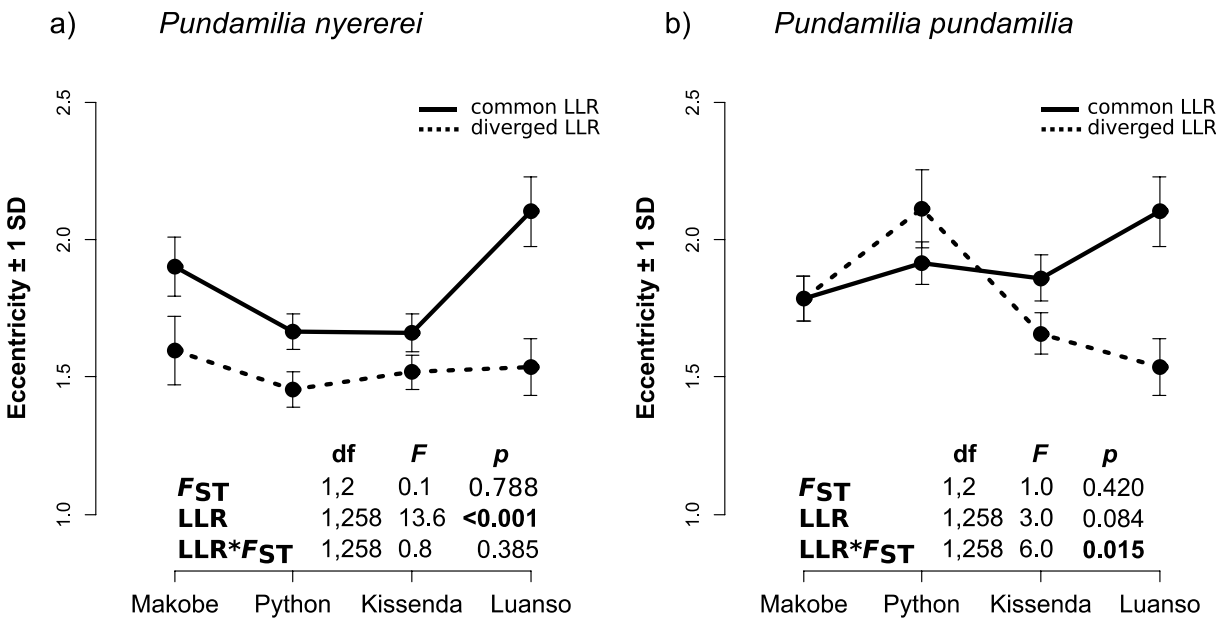

Figure 3:

Average eccentricity (± 1 SD) of all pairwise trait matrix comparisons that either showed a significantly diverged line of least resistance (LLR; dashed line) or share a common LLR (solid line) for a) *Pundamilia nyererei* and b) *P. pundamilia* separately for each island. In addition, the results of a linear mixed effects model are given, testing for a statistical association of eccentricity with either the degree of interspecific gene flow (F_{ST}), the number of diverged/undiverged LLR and its interaction. For Luanso Islands the same *Pundamilia* hybrids were used.

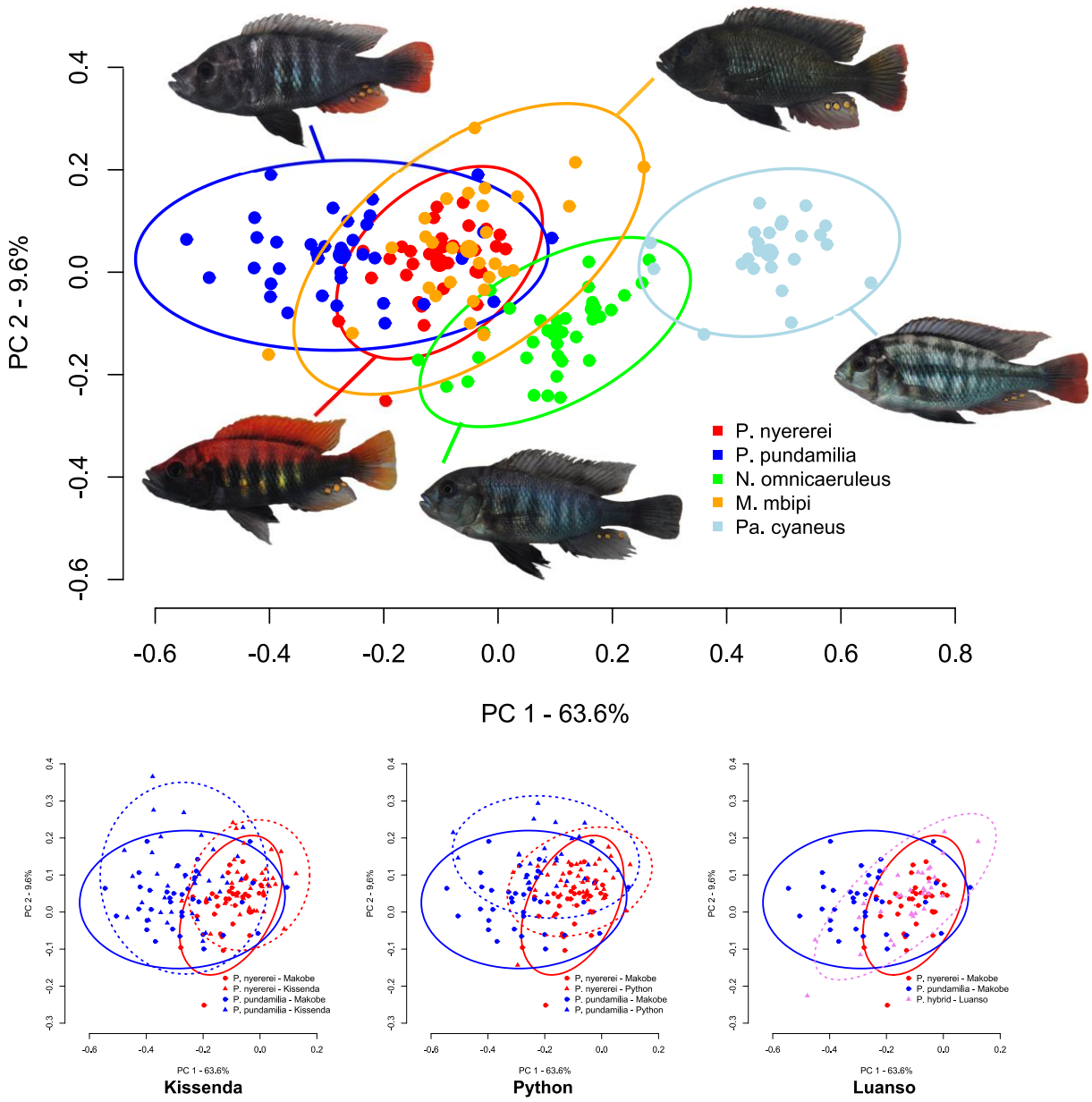

Figure 4:

Individual PC scores for the studied species assembledge from Makobe Island in a common morphospace (top). The ellipses indicate the 95% confidence boundaries for each species and represent the underlying **P** matrix (red - *P. nyererei,* blue - *P. pundamilia*, orange - *M. mbipi*, green - *N. omnicaeruleus*, light blue - *Pa. cyaneus*). The bottom panels give the position of *Pundamilia* specimens projected into the common morphospace of the Makobe species community (only *P. pundamilia* and *P*. nyererei are shown) for Kissenda and Python as well

as the *Pundamilia* hybrid individuals in Luanso. Dashed lines represent the 95% confidence boundaries of the projected individuals for each island.

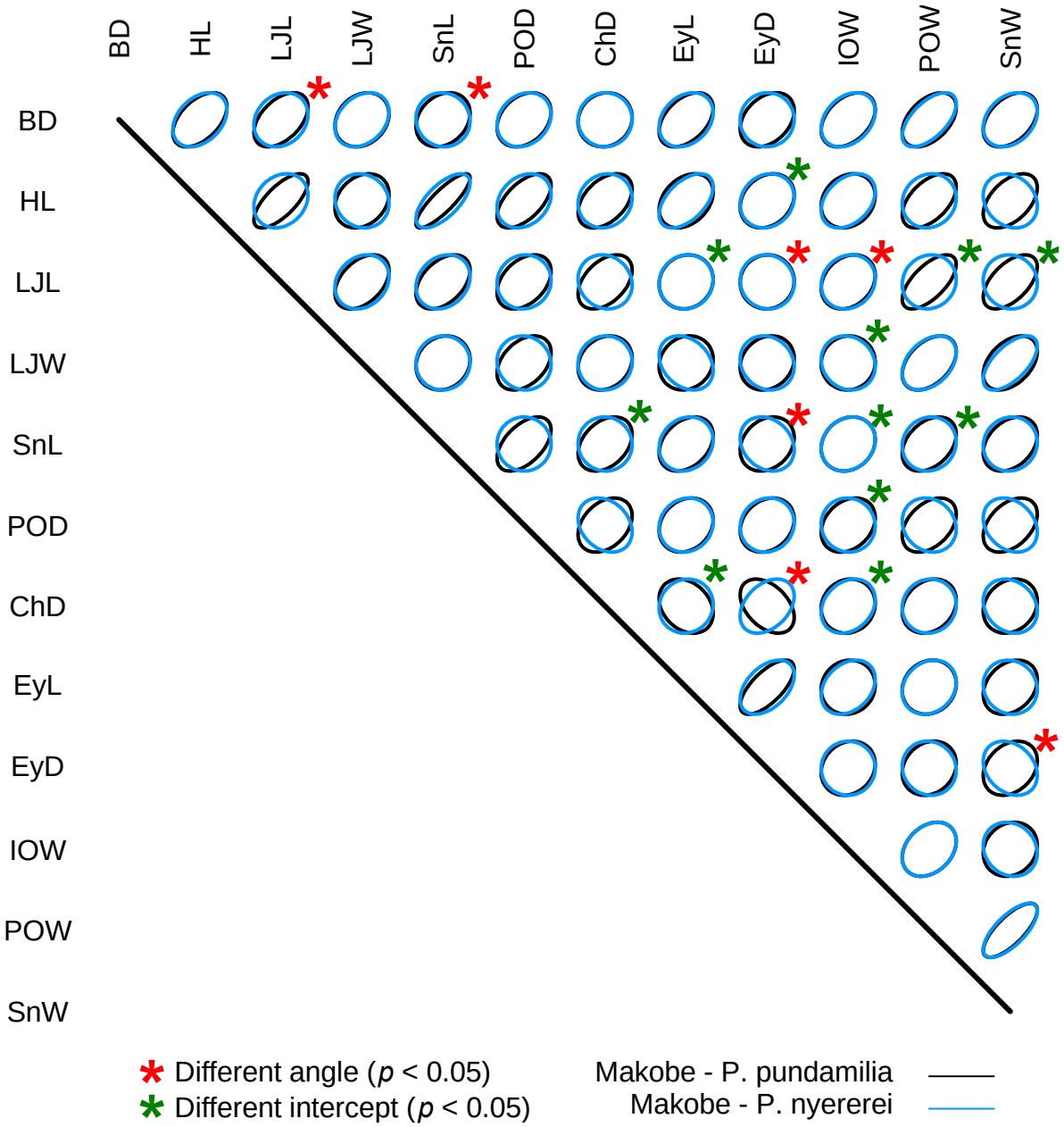

Figure S1

A comparison of trait by trait covariances for *Pundamilia pundamilia* (ellipses in black) and *P. nyereri* (ellipses in blue) from Makobe Island. Covariances are scaled, hence only the differences in shape are shown. Red asterisks mark instances where the angle of the underlying LLR differs significantly ($p < 0.05$) between species, whereas green asterisks depict cases where the intercept differs between species. Abbreviations are as follow: BD - body depth, HL - head length, LJL - lower jaw length, LJW - lower jaw width, SnL - snout length, POD -

preorbital depth, ChD - cheek depth, EyL - eye length, EyD - eye depth, IOW - interorbital width, POW - preorbital width, SnW - snout width.

Table 1: Sampling summary

Number of specimens per species and island included in the analyses.

	Makobe	**Python**	**Kissenda**	**Luanso**
Pundamilia pundamilia	36	26	35	-
Pundamilia nyererei	35	35	35	-
Pundamilia "hybrid"	-	-	-	35
Neochromis omnicaeruleus	35	-	-	-
Paralabidochromis cyaneus	24	-	-	-
Mbipia mbipi	29	-	-	-

Table S1

Summary of the calculated values for each species and island for each trait-by-trait **P** matrix. Given are the traits involved in each pair (Trait 1 and 2) followed by a summary if the line of least resistance (LLR) is shared or diverged between *P. nyererei* and *P. pundamilia* at Makobe Island. For Makobe Island, the eccentricity of each trait-by-trait **P** matrix is given for each species as well as the angle (°) and intercept between the two **P** matrices together with their associated *p* values are provided. *P* values are based on a bootstrap approach with 1000 replicates. For all other species from Python, Kissenda and Luanso, the respective eccentricity values are provided (see main text for details).

			Makobe						Python		Kissenda		
			Eccentricity		Angle		Intercept		Eccentricity		Eccentricity		Luanso
Trait 1	Trait 1	LLR	*P. nyererei*	*P. pundamilia*	°	*p*		*p*	*P. nyererei*	*P. pundamilia*	*P. nyererei*	*P. pundamilia*	*P.* "hybrid"
BD	ChD	shared	1.6800	1.7415	3.39	0.775	2.29	0.114	1.4305	2.4000	1.5608	2.0726	1.3213
BD	EyD	shared	1.4113	1.4465	35.58	0.303	0.01	0.385	1.0977	1.5911	1.0849	1.5088	1.2132
BD	EyL	shared	1.6497	1.6036	35.91	0.610	0.04	0.368	1.1709	1.6668	1.1516	1.2825	1.3982
BD	HL	shared	2.9328	1.7296	30.68	0.651	0.07	0.238	1.6139	1.3471	1.6459	1.6818	1.7996
BD	IOW	shared	1.4880	1.5598	29.97	0.584	0.05	0.596	1.5143	1.5753	1.6038	1.8054	1.4391
BD	LJL	diverged	1.4624	2.3990	58.30	0.002	0.11	0.750	1.8589	2.9217	1.2458	2.2629	1.7639
BD	LJW	shared	1.6259	2.0864	10.04	0.285	0.09	0.842	2.1688	2.9589	1.7341	2.8081	3.2562
BD	POD	shared	1.3135	1.6238	47.41	0.124	0.08	0.683	1.4352	2.4706	1.3116	1.8814	1.2070
BD	POW	shared	2.0029	1.9050	27.58	0.524	0.03	0.822	2.2966	1.8027	1.8720	2.0214	1.9264
BD	SnL	diverged	1.1894	1.7124	85.56	0.000	0.13	0.652	1.1553	1.8481	1.2423	1.5730	1.4582
BD	SnW	shared	1.4655	1.9352	6.10	0.731	0.03	0.922	1.7060	1.9498	1.5265	1.7017	2.4841
ChD	EyD	diverged	2.6216	2.2495	25.60	0.000	0.02	0.066	1.4229	1.7960	1.6161	1.7865	1.4106
ChD	EyL	diverged	2.5541	1.6970	16.74	0.167	0.05	0.000	1.2975	2.2163	1.7822	2.0419	1.0329
ChD	IOW	diverged	2.2161	1.4874	2.14	0.885	0.05	0.002	1.3050	2.2247	1.4075	1.4808	1.1142
ChD	POW	shared	1.9291	1.3058	24.66	0.232	0.01	0.732	1.2108	1.8874	1.6001	1.9696	1.1935
ChD	SnW	shared	1.4110	1.2229	54.88	0.273	0.02	0.620	1.0715	2.1878	1.0731	1.3780	1.7683
EyD	IOW	shared	1.1200	1.3735	12.97	0.577	0.17	0.411	1.5423	1.1935	1.2481	1.7109	1.5400

EyD	POW	shared	1.2474	1.7149	18.49	0.291	0.13	0.586	1.9324	1.6237	1.1707	1.2717	1.7673
EyD	SnW	diverged	1.9034	1.9703	22.61	0.042	0.08	0.831	1.4247	1.5610	1.8393	1.4452	2.6805
EyL	EyD	shared	1.6205	2.3863	14.19	0.707	0.02	0.151	2.5160	2.5405	2.5386	2.4568	2.3979
EyL	IOW	shared	1.4322	1.1011	1.98	0.968	0.12	0.285	1.4340	1.1208	1.5352	1.5398	1.5013
EyL	POW	shared	1.4025	1.3740	4.97	0.882	0.14	0.368	1.6073	1.5576	1.0724	1.1902	1.2523
EyL	SnW	shared	1.9329	1.6246	20.77	0.201	0.03	0.931	1.3067	1.5742	1.5123	1.5657	1.8111
HL	ChD	shared	4.5425	2.2441	14.82	0.196	0.57	0.432	1.8818	2.5670	2.6336	3.1606	1.9790
HL	EyD	diverged	1.9377	1.2644	41.40	0.203	0.13	0.013	1.8565	1.7419	1.7200	1.4457	1.4502
HL	EyL	shared	2.2887	1.4736	9.60	0.901	0.09	0.211	1.7015	2.1215	1.9886	1.3315	2.3066
HL	IOW	shared	2.3491	1.3781	7.47	0.892	0.26	0.232	1.6607	1.0987	2.3177	1.8743	2.0432
HL	LJL	shared	2.0112	3.4175	11.82	0.343	0.14	0.799	2.6708	3.2319	1.8448	3.1511	2.6928
HL	LJW	shared	3.9548	2.3129	9.49	0.318	0.03	0.963	2.2455	2.5582	2.8265	3.4245	5.1003
HL	POD	shared	2.3447	2.2792	16.99	0.465	0.13	0.738	1.9795	2.4889	2.0686	2.6832	1.8297
HL	POW	shared	2.3652	2.1554	19.46	0.577	0.27	0.335	2.3280	1.6419	1.6436	2.3806	2.4618
HL	SnL	shared	3.3050	4.1555	9.64	0.548	0.05	0.912	2.6480	3.7118	3.0239	3.1088	3.0536
HL	SnW	shared	3.4773	2.2459	22.86	0.185	0.01	0.976	1.9551	1.9013	2.2706	2.2243	3.7312
IOW	POW	shared	1.3942	1.4800	9.89	0.876	0.10	0.348	1.6877	2.0630	1.3964	1.6280	1.1655
IOW	SnW	shared	1.6322	1.4438	20.88	0.394	0.19	0.463	1.2128	1.8510	1.1229	1.3574	1.7743
LJL	ChD	shared	2.3533	1.6311	56.38	0.366	0.59	0.157	1.6551	1.9506	2.1198	1.4358	1.3243
LJL	EyD	diverged	1.0517	2.1984	36.23	0.000	0.02	0.227	2.0877	3.1990	1.5813	1.8348	1.8788
LJL	EyL	diverged	1.1161	1.7871	13.96	0.235	0.04	0.048	1.5892	2.8747	1.6127	1.8864	1.4072
LJL	IOW	diverged	1.1743	1.7747	51.06	0.014	0.01	0.639	1.5669	2.7815	1.9314	1.4115	1.3172
LJL	LJW	shared	2.0964	1.5710	35.96	0.403	0.22	0.720	1.8034	1.2464	2.1290	1.4518	2.2449
LJL	POD	shared	1.1692	1.6746	53.76	0.160	0.18	0.066	1.5822	1.5810	1.5605	1.1898	1.9661
LJL	POW	diverged	1.2356	2.2884	45.36	0.057	0.10	0.024	1.6574	2.1697	1.2524	1.7810	1.6301
LJL	SnL	shared	1.2961	1.6570	32.02	0.599	0.08	0.552	1.2424	1.6229	1.4816	1.4273	1.6130
LJL	SnW	diverged	1.7620	1.9214	57.26	0.274	0.72	0.047	1.3750	1.5160	1.7682	1.3296	1.4950

LJW	ChD	shared	1.1532	1.2694	58.80	0.171	0.34	0.054	1.3239	1.7384	1.3044	1.4430	2.4031
LJW	EyD	shared	2.0945	2.2917	9.65	0.147	0.01	0.525	1.6220	2.2539	1.6895	2.4357	3.4553
LJW	EyL	shared	2.3529	1.8389	14.71	0.091	0.01	0.383	1.4757	2.2439	1.8612	2.5707	2.4639
LJW	IOW	diverged	1.8665	1.7109	7.77	0.491	0.06	0.008	1.3726	2.6093	1.3939	1.9560	2.3627
LJW	POD	shared	1.7588	1.6894	27.11	0.141	0.00	0.925	1.3870	1.5121	1.6030	1.4955	2.8191
LJW	POW	shared	1.9297	1.7353	9.72	0.436	0.03	0.189	1.9412	1.7690	1.7062	2.2895	3.1164
LJW	SnL	shared	1.7304	1.2902	13.09	0.631	0.06	0.301	1.3003	1.5377	1.5579	1.9997	3.4399
LJW	SnW	shared	2.0867	1.6370	6.35	0.811	0.01	0.907	2.8071	2.0079	1.3429	1.6819	2.9909
POD	ChD	shared	2.1235	1.4918	39.95	0.234	0.15	0.259	1.3598	1.6251	1.4346	1.1665	1.3569
POD	EyD	shared	1.2011	1.7099	1.22	0.903	0.01	0.414	1.4526	1.7626	1.1526	1.6140	1.2921
POD	EyL	shared	1.2913	1.4032	6.26	0.769	0.02	0.139	1.2040	1.7985	1.3022	1.7509	1.1263
POD	IOW	diverged	1.0635	1.4260	42.64	0.285	0.06	0.031	1.4004	2.4585	1.8469	1.3014	1.2485
POD	POW	shared	1.1659	1.5347	80.44	0.063	0.02	0.274	1.4789	1.5001	1.6952	1.5897	1.3546
POD	SnW	shared	1.6411	1.5663	51.61	0.342	0.10	0.212	1.1844	1.7238	1.2271	1.1412	1.9997
POW	SnW	shared	2.6449	2.6560	10.30	0.780	0.02	0.905	2.1807	1.7061	2.1443	1.9231	3.7131
SnL	ChD	diverged	1.9866	1.4600	39.60	0.453	2.46	0.021	1.1366	1.5446	1.3942	1.9028	1.2200
SnL	EyD	diverged	1.3260	1.8948	35.82	0.001	0.01	0.290	1.2805	1.5537	1.2976	1.2613	1.4525
SnL	EyL	shared	1.3370	1.6602	5.69	0.699	0.01	0.585	1.2429	1.7585	1.2377	1.4466	1.0452
SnL	IOW	diverged	1.1922	1.4279	21.76	0.357	0.08	0.009	1.0510	1.7112	1.2863	1.2006	1.0848
SnL	POD	shared	1.0139	1.8042	43.53	0.402	0.02	0.459	1.4782	2.1669	1.4357	1.4802	1.3761
SnL	POW	diverged	1.0901	1.4760	16.44	0.597	0.07	0.022	1.3502	1.3068	1.1044	1.9278	1.6380
SnL	SnW	shared	1.5052	1.4065	38.63	0.569	0.35	0.051	1.1543	1.7254	1.3152	1.6208	2.4303

Table S2

Residuals of the two leading principal component (PC) axes based on size corrected linear measurements of specimens from Makobe Island. Abbreviations are as follow: BD - body depth, HL - head length, LJL - lower jaw length, LJW - lower jaw width, SnL - snout length, POD - preorbital depth, ChD - cheek depth, EyL - eye length, EyD - eye depth, IOW - interorbital width, POW - preorbital width, SnW - snout width.

	PC1 - 63.6%	PC2 - 9.6%
BD	-0.105	-0.096
HL	-0.217	-0.208
LJL	-0.558	-0.353
LJW	-0.443	0.588
SnL	-0.271	-0.172
POD	-0.207	-0.094
ChD	-0.339	-0.447
EyL	-0.070	-0.021
EyD	-0.047	0.009
IOW	-0.138	0.243
POW	-0.301	0.268
SnW	-0.294	0.327

Table S3

Summary of a TukeyHSD *post hoc* decomposition of an ANOVA using the principal component (PC) scores along the first and second axis for all specimens at Makobe Island. Given are the species contrasts followed by the adjusted p value (see main text for details).

Species 1	**Species 2**	***p - PC1***	***p - PC2***
M. mbipi	*Pa. Cyaneus*	<0.001	0.998
P. nyererei	*Pa. Cyaneus*	<0.001	0.882
N. omnicaeruleus	*Pa. Cyaneus*	<0.001	<0.001
P. pundamilia	*Pa. Cyaneus*	<0.001	1.000
P. nyererei	*M. mbipi*	0.297	0.662
N. omnicaeruleus	*M. mbipi*	<0.001	<0.001
P. pundamilia	*M. mbipi*	<0.001	0.977
N. omnicaeruleus	*P. nyererei*	<0.001	<0.001
P. pundamilia	*P. nyererei*	<0.001	0.927
P. pundamilia	*N. omnicaeruleus*	<0.001	<0.001

References

Abbott, R., D. Albach, S. Ansell, J. W. Arntzen, S. J. E. Baird, N. Bierne, J. W. Boughman, A. Brelsford, C. A. Buerkle, R. Buggs, R. K. Butlin, U. Dieckmann, F. Eroukhmanoff, A. Grill, S. H. Cahan, J. S. Hermansen, G. Hewitt, A. G. Hudson, C. Jiggins, J. Jones, B. Keller, T. Marczewski, J. Mallet, P. Martinez-Rodriguez, M. Möst, S. Mullen, R. Nichols, A. W. Nolte, C. Parisod, K. Pfennig, A. M. Rice, M. G. Ritchie, B. Seifert, C. M. Smadja, R. Stelkens, J. M. Szymura, R. Vainola, J. B. W. Wolf, & D. Zinner, 2013. Hybridization and speciation. Journal of evolutionary Biology 26: 229–246.

Arnold, S. J., & P. C. Phillips, 1999. Hierarchical comparison of genetic variance-covariance matrices. II. Coastal-inland divergence in the garter snake, *Thamnophis elegans*. Evolution 53: 1516–1527.

Arnold, S. J., R. Bürger, P. A. Hohenlohe, B. C. Ajie, & A. G. Jones, 2008. Understanding the evolution and stability of the G-matrix. Evolution 62: 2451–2461.

Bailey, R. I., F. Eroukhmanoff, & G.-P. Sætre, 2013. Hybridization and genome evolution II: Mechanisms of species divergence and their effects on evolution in hybrids. Current Zoology 59: 675–685.

Barel, C. D. N., M. vanOijen, F. Witte, & E. Wittemaas, 1977. An introduction to taxonomy and morphology of haplochromine cichlidae from Lake Victoria. Netherlands Journal of Zoology 27: 333–380.

Berner, D., 2009. Correction of a bootstrap approach to testing for evolution along lines of least resistance. Journal of Evolutionary Biology 22: 2563–2565.

Blows, M. W., S. L. Allen, J. M. Collet, S. F. Chenoweth, & K. McGuigan, 2015. The phenome-wide distribution of genetic variance. American Naturalist 186: 15–30.

Calsbeek, B., S. Lavergne, M. Patel, & J. Molofsky, 2011. Comparing the genetic architecture and potential response to selection of invasive and native populations of reed canary grass. Evolutionary Applications 4: 726–735.

Chapuis, E., G. Martin, & J. Goudet, 2008. Effects of selection and drift on G matrix evolution in a heterogeneous environment: a multivariate Qst-Fst Test with the freshwater snail *Galba truncatula*. Genetics 180: 2151–2161.

Cheverud, J. M., 1988. A Comparison of genetic and phenotypic correlations. Evolution 42: 958–968.

Draghi, J. A., & M. C. Whitlock, 2012. Phenotypic plasticity facilitates mutational variance, genetic variance, and evolvability along the major axis of environmental variation. Evolution 66: 2891–2902.

Eroukhmanoff, F., 2009. Just how much is the G-matrix actually constraining adaptation? Evolutionary Biology 36: 323–326.

Eroukhmanoff, F., & E. I. Svensson, 2008. Phenotypic integration and conserved covariance structure in calopterygid damselflies. Journal of Evolutionary Biology 21:

514–526.

Eroukhmanoff, F., & E. I. Svensson, 2011. Evolution and stability of the G-matrix during the colonization of a novel environment. Journal of Evolutionary Biology 24: 1363–1373.

Falconer, D. S., 1989. Introduction to quantitative genetics. John Wiley & Sons, New York.

Fox, J., & S. Weisberg, 2011. An R Companion to Applied Regression. Sage Publications Inc., Thousand Oaks.

Gilman, R. T., & J. E. Behm, 2011. Hybridization, species collapse, and species reemergence after disturbance to premating mechanisms of reproductive isolation. Evolution 65: 2592–2605.

Grant, P. R., & B. R. Grant, 1994. Phenotypic and genetic effects of hybridization in Darwin's finches. Evolution 48: 297–316.

Greg, S., 2015. Lake Victoria Shapefiles. figshare. https://dx.doi.org/10.6084/m9.figshare.1494839.v1

Guillaume, F., & M. C. Whitlock, 2007. Effects of migration on the genetic covariance matrix. Evolution 61: 2398–2409.

Hine, E., S. F. Chenoweth, H. D. Rundle, & M. W. Blows, 2009. Characterizing the evolution of genetic variance using genetic covariance tensors. Philosophical Transactions of the Royal Society of London Series B, Biological Sciences 364: 1567–1578.

Jones, A. G., S. J. Arnold, & R. Borger, 2003. Stability of the G-matrix in a population experiencing pleiotropic mutation, stabilizing selection, and genetic drift. Evolution 57: 1747–1760.

Kirkpatrick, M., 2009. Patterns of quantitative genetic variation in multiple dimensions. Genetica 136: 271–284.

Klingenberg, C. P., 2010. Evolution and development of shape: integrating quantitative approaches. Nature Reviews Genetics 11: 623–635.

Lande, R., 1979. Quantitative genetic analysis of multivariate evolution, applied to brain:body size allometry. Evolution 33: 402–416.

Lande, R., 2009. Adaptation to an extraordinary environment by evolution of phenotypic plasticity and genetic assimilation. Journal of Evolutionary Biology 22: 1435–1446.

Lande, R., & S. J. Arnold, 1983. The measurement of selection on correlated characters. Evolution 37: 1210–1226.

Lucek, K., A. Sivasundar, B. K. Kristjánsson, S. Skulason, & O. Seehausen, 2014a. Quick divergence but slow convergence during ecotype formation in lake and stream stickleback pairs of variable age. Journal of Evolutionary Biology 27: 1878–1892.

Lucek, K., M. Lemoine, & O. Seehausen, 2014b. Contemporary ecotypic divergence during a recent range expansion was facilitated by adaptive introgression. Journal of

90 Evolutionary Biology 27: 2233–2248.

91 Lucek, K., A. Sivasundar, & O. Seehausen, 2014c. Disentangling the role of phenotypic
92 plasticity and genetic divergence in contemporary ecotype formation during a biological
93 invasion. Evolution 68: 2619–2632.

94 Magalhaes, I. S., S. Mwaiko, M. V. Schneider, & O. Seehausen, 2009. Divergent selection
95 and phenotypic plasticity during incipient speciation in Lake Victoria cichlid fish. Journal
96 of Evolutionary Biology 22: 260–274.

97 Mallet, J., 2007. Hybrid speciation. Nature 446: 279–283.

98 Meier, J. I., V. C. Sousa, D. A. Marques, O. M. Selz, C. E. Wagner, L. Excoffier, & O.
99 Seehausen. Demographic modeling of whole genome data reveals parallel origin of
100 similar *Pundamilia* cichlid species after hybridization. submitted.

101 Nolte, A. W., J. Freyhof, K. Stemshorn, & D. Tautz, 2005. An invasive lineage of sculpins,
102 *Cottus* sp (*Pisces, Teleostei*) in the Rhine with new habitat adaptations has originated
103 from hybridization between old phylogeographic groups. Proceedings of the Royal
104 Society of London Series B, Biological Sciences 272: 2379–2387.

105 Orr, H. A., 2005. The genetic theory of adaptation: a brief history. Nature Reviews
106 Genetics 6: 119–127.

107 Parsons, K. J., Y. H. Son, & R. C. Albertson, 2011. Hybridization promotes evolvability in
108 african cichlids: connections between transgressive segregation and phenotypic
109 integration. Evolutionary Biology 38: 306–315.

110 Reist, J. D., 1986. An empirical evaluation of coefficients used in residual and allometric
111 adjustment of size covariation. Canadian Journal Of Zoology 64: 1363–1368.

112 Renaud, S., P. Alibert, & J.-C. Auffray, 2012. Modularity as a source of new morphological
113 variation in the mandible of hybrid mice. BMC Evolutionary Biology 12: 141.

114 Rieseberg, L. H., O. Raymond, D. M. Rosenthal, Z. Lai, K. Livingstone, T. Nakazato, J. L.
115 Durphy, A. E. Schwarzbach, L. A. Donovan, & C. Lexer, 2003. Major ecological transitions
116 in wild sunflowers facilitated by hybridization. Science 301: 1211–1216.

117 Roseman, C. C., 2016. Random genetic drift, natural selection, and noise in human cranial
118 evolution. American Journal of Physical Anthropology. DOI: 10.1002/ajpa.22918

119 Rudman, S. M., & D. Schluter, 2016. Ecological impacts of reverse speciation in
120 threespine stickleback. Current biology 26: 490–495.

121 Schluter, D., 1996. Adaptive radiation along genetic lines of least resistance. Evolution
122 50: 1766–1774.

123 Schluter, D., 2000. The Ecology of Adaptive Radiation. Oxford University Press, Oxford.

124 Seehausen, O., 2004. Hybridization and adaptive radiation. Trends in Ecology and
125 Evolution 19: 198–207.

Seehausen, O., 2006. African cichlid fish: a model system in adaptive radiation research. Proceedings of the Royal Society of London Series B, Biological Sciences 273: 1987–1998.

Seehausen, O., & N. Bouton, 1997. Microdistribution and fluctuations in niche overlap in a rocky shore cichlid community in Lake Victoria. Ecology of Freshwater Fish 6: 161–173.

Seehausen, O., E. Lippitsch, N. Bouton, & H. Zwennes, 1998. *Mbipi*, the rock-dwelling cichlids of Lake Victoria: description of three new genera and fifteen new species (*Teleostei*). Ichthyological Exploration of Freshwaters 9: 129–228.

Seehausen, O., J. vanAlphen, & F. Witte, 1997. Cichlid fish diversity threatened by eutrophication that curbs sexual selection. Science 277: 1808–1811.

Seehausen, O., R. K. Butlin, I. Keller, C. E. Wagner, J. W. Boughman, P. A. Hohenlohe, C. L. Peichel, G.-P. Saetre, C. Bank, Å. Brännström, A. Brelsford, C. S. Clarkson, F. Eroukhmanoff, J. L. Feder, M. C. Fischer, A. D. Foote, P. Franchini, C. D. Jiggins, F. C. Jones, A. K. Lindholm, K. Lucek, M. E. Maan, D. A. Marques, S. H. Martin, B. Matthews, J. I. Meier, M. Möst, M. W. Nachman, E. Nonaka, D. J. Rennison, J. Schwarzer, E. T. Watson, A. M. Westram, & A. Widmer, 2014. Genomics and the origin of species. Nature Reviews Genetics 15: 176–192.

Seehausen, O., Y. Terai, I. S. Magalhaes, K. L. Carleton, H. D. J. Mrosso, R. Miyagi, I. van der Sluijs, M. V. Schneider, M. E. Maan, H. Tachida, H. Imai, & N. Okada, 2008. Speciation through sensory drive in cichlid fish. Nature 455: 620–626.

Selz, O. M., K. Lucek, K. A. Young, & O. Seehausen, 2014. Relaxed trait covariance in interspecific cichlid hybrids predicts morphological diversity in adaptive radiations. Journal of Evolutionary Biology 27: 11–24.

Stelkens, R. B., M. A. Brockhurst, G. D. D. Hurst, & D. Greig, 2014. Hybridization facilitates evolutionary rescue. Evolutionary Applications 7: 1209–1217.

Stelkens, R., & O. Seehausen, 2009. Genetic distance between species predicts novel trait expression in their hybrids. Evolution 63: 884–897.

Steppan, S., P. C. Phillips, & D. Houle, 2002. Comparative quantitative genetics: evolution of the G matrix. Trends in Ecology and Evolution 17: 320–327.

Taylor, E. B., J. W. Boughman, M. Groenenboom, M. Sniatynski, D. Schluter, & J. L. Gow, 2006. Speciation in reverse: morphological and genetic evidence of the collapse of a three-spined stickleback (*Gasterosteus aculeatus*) species pair. Molecular Ecology 15: 343–355.

Vonlanthen, P., D. Bittner, A. G. Hudson, K. A. Young, R. Müller, B. Lundsgaard-Hansen, D. Roy, S. Di Piazza, C. R. Largiadèr, & O. Seehausen, 2012. Eutrophication causes speciation reversal in whitefish adaptive radiations. Nature 482: 357–362.

Wood, C. W., & E. D. Brodie, 2015. Environmental effects on the structure of the G-matrix. Evolution 69: 2927–2940.

Wright, S., 1932. The roles of mutation, inbreeding, crossbreeding and selection in evolution. Proceedings of the sixth international congress of genetics: 356-366.